

DEEP CCD PHOTOMETRY OF OLD OPEN CLUSTERS

MARC KASSIS

Willamette University, 900 State Street, Salem, Oregon 97301; and Boston University, 725 Commonwealth Avenue, Boston, Massachusetts 02215

Electronic mail: mkassis@hyades.bu.edu

KENNETH A. JANES

Department of Astronomy, Boston University, 725 Commonwealth Avenue, Boston, Massachusetts 02215

Electronic mail: janes@hyades.bu.edu

EILEEN D. FRIEL

Department of Astronomy, Boston University, 725 Commonwealth Avenue, Boston, Massachusetts 02215; and Maria Mitchell Observatory, 3 Vestal Street, Nantucket, Massachusetts 02554

Electronic mail: friel@hyades.bu.edu

RANDY L. PHELPS¹

The Observatories of the Carnegie Institution of Washington, 813 Santa Barbara Street, Pasadena, California 91101

Electronic mail: phelps@ociw.edu

Received 1996 August 20; revised 1997 January 28

ABSTRACT

Ages and distance moduli for the open clusters NGC 2204, Berkeley 39, NGC 2477, and Melotte 66 are constrained by comparing the theoretical models developed by Bertelli *et al.* (1994, A&A, 106, 235) to the observed cluster color-magnitude diagrams which are based on deep CCD photometry. Out of a set of comparison models, no single isochrone was superior to the others in describing an observed color-magnitude diagram. Thus, a best fitting model was selected based not only on the match to an observed color-magnitude diagram, but also on the isochrone's agreement with adopted values for the cluster's metallicity and reddening. The range of otherwise acceptable models help quantify the age and distance modulus uncertainty of each cluster. Based on the best fitting models NGC 2204 is $1.6_{-0.3}^{+0.9}$ Gyr old with $(m-M)_o = 13.0_{-0.4}^{+0.5}$, Berkeley 39 has an age of 6_{-1}^{+2} Gyr with $(m-M)_o = 12.9 \pm 0.2$, NGC 2477 is $1_{-0.2}^{+0.3}$ Gyr old with $(m-M)_o = 10.5_{-0.3}^{+0.4}$, and Melotte 66 has an age of 4 ± 1 Gyr with $(m-M)_o = 13.2_{-0.1}^{+0.3}$. © 1997 American Astronomical Society. [S0004-6256(97)02005-0]

1. INTRODUCTION

The Galaxy's system of open star clusters is one instrument through which we may examine and probe the formation and evolution of the Galactic disk. As a small subset of the open cluster system, the old open clusters (those with ages as old as or older than 800 Myr) allow us to explore the history of star and cluster formation over a wide range of the Galaxy's lifetime. Recently, surveys to find and identify members of the old open cluster system (Phelps *et al.* 1994) have led to an increased number of detailed studies of the old cluster population (Kaluzny & Richtler 1989; Kassis *et al.* 1996; MacMinn *et al.* 1994; Montgomery *et al.* 1994; Phelps & Janes 1996). There is now a significant sample to investigate the chemical evolution of the Galaxy (Friel & Janes 1993; Friel 1995) and the age distribution of open clusters (Janes & Phelps 1994). Studies of the oldest known open cluster, Berkeley 17, with an age of 12 Gyr (Phelps *et al.*

1995; Kaluzny 1994), help constrain time scales for halo collapse models and the initial stage of formation of the Galactic disk (Janes & Phelps 1994).

The traditional method of deriving an age for a cluster involves comparing theoretical stellar evolutionary models to the observed cluster color-magnitude diagrams (CMD). The metallicity and reddening values are usually assumed while the age and distance modulus are constrained through comparisons of theoretical isochrones. This method for comparing isochrones involves the investigator's judgment in choosing which models compare well to an observed CMD. A similar method for estimating the age of an open cluster with the use of a CMD is to examine the differences between the magnitude and color of the turnoff and positions along the giant branch (Anthony-Twarog & Twarog 1985; Janes & Phelps 1994; Phelps *et al.* 1994).

Recently, a different approach has been taken to generate synthetic CMDs to compare with observed CMDs (Carraro *et al.* 1993; Carraro *et al.* 1994; Gozzoli *et al.* 1996). This fresh approach to comparing isochrones shows what the models would look like given assumed observational errors

¹Visiting Astronomer, Cerro Tololo Inter-American Observatory. CTIO is operated by AURA, Inc., under contract to the National Science Foundation.

TABLE 1. Observations.

Cluster/date	Filter	Frames:exposure time (s)
NGC 2477 5/6 April 94	<i>U</i>	1:60, 4:450
	<i>B</i>	1:5, 1:30, 5:240
	<i>V</i>	1:5, 1:30, 5:180
	<i>I</i>	1:2, 1:30, 8:100
NGC 2204 6/7 April 94	<i>B</i>	2:30, 6:150
	<i>V</i>	1:2, 1:5, 3:20, 4:240
	<i>I</i>	1:1, 1:2, 6:120
Berkeley 39 8/9 April 94	<i>U</i>	4:450
	<i>B</i>	3:20, 4:375
	<i>V</i>	3:20, 5:300
	<i>I</i>	3:13, 5:200
Melotte 66 8/9 April 94	<i>V</i>	3:2, 3:20, 4:300
	<i>I</i>	3:2, 3:300

and binary star contributions. The synthetic CMD method, like the traditional method of comparing theoretical isochrones, relies on the investigator's judgment to differentiate between an unacceptable and acceptable match. Thus, the age determinations from synthetic and traditional isochrone comparison methods rely on the investigator's selection of a best fitting model and are often left unquantified.

In the current paper, we present CMDs of four open clusters to which we compare Bertelli *et al.* (1994) isochrones using the traditional method. To constrain the ages and distance moduli, models ranging in age and metallicity are matched to cluster CMDs based on deep CCD photometry. Refining the estimates of clusters' ages and distance moduli are important because they help us understand the history of star formation and consequently the evolution of the galactic disk.

In Sec. 2, the reduction process is described. Values for the reddening and metallicity are adopted from the literature in Sec. 3, and the clusters' *V*, *V-I* CMDs based on deep photometry are presented. Section 4 describes the method of selecting isochrone models as acceptable comparisons to the observed CMDs and presents a discussion of our best fitting models. A summary is provided in the final section.

2. OBSERVATIONS AND REDUCTIONS

Deep photometry for the open clusters NGC 2477, NGC 2204, Berkeley 39, and Melotte 66 was obtained during a five night observing program at the 1.5 m telescope at Cerro Tololo Inter-American Observatory, 1994 April. A Tek 2048² CCD with quad readout and readnoise of $4e^-$ provided a 14.7×14.7 arcmin field of view. In Table 1, the number of observations for a given filter and exposure time are listed for each cluster. Note that only Berkeley 39 and NGC 2477 were observed in all passbands and that all clusters have *V* and *I* photometry.

Standard procedures within the IRAF² data reduction soft-

ware package were followed in processing the photometry. Because the Tek CCD had a quad readout, variations from quadrant to quadrant exist; however, overscan, bias, and flat-field corrections eliminated these variations to better than one percent. For the five night run, a combined 26 sky flats in the *U* passband, 23 in *B*, 17 in *V*, and 21 in *I* were used to flat-field the object and standard fields.

Instrumental magnitudes for the clusters were obtained using a quadratically varying point spread function under the DIGIPHOT/IRAF routine. The instrumental magnitudes were transformed to the Landolt (1992) system of standards plus standards in the dipper asterism of M67 (Montgomery *et al.* 1993). A total of 89 standards were used in the transformation ranging in color from -0.271 to 2.326 ($B-V$) over an airmass range of 1.074 to 2.003.

Two solutions to the transformation equations were used to transform our instrumental magnitudes. The first set (below) is a three-color solution, to transform the *U*, *B*, and *V* colors of stars with both *B* and *V* measures, where X is the airmass and lower case letters are instrumental magnitudes.

$$u = V + (B - V) + 4.2051 + 0.4155X + 0.9288(U - B),$$

$$b = V + 2.2331 + 0.2598X + 1.1148(B - V)$$

$$- 0.03X(B - V),$$

$$v = V + 2.0899 + 0.1185X - 0.0304(B - V).$$

A second set of transformation equations was employed to transform the *V* and *I* indices. Because observations in the *B* passband do not extend to magnitudes as faint as those observed in *V* and *I*, the following equations were used to match stars in the *V* and *I* passband so that fainter stars were transformed.

$$v = V + 2.0870 + 0.1214X + 0.0293(V - I),$$

$$i = V + 3.0586 + 0.0744X - 1.0131(V - I).$$

Fifteen hundred stars that were transformed under both sets of equations were used to test consistency in the two solutions for *V* between the two equation sets. The *V* magnitudes for stars matched between transformations differed by a mean of 0.003 *V* mag with a standard deviation of 0.007 *V* mag, in the sense of $V(VI \text{ transformation}) - V(UBV \text{ transformation})$.

3. CLUSTER PROPERTIES AND CMD FEATURES

The *V*, *V-I* CMDs for all clusters are presented in Fig. 1, while Fig. 2 presents the *V*, $B-V$ CMDs for the three clusters with *BV* photometry. Notice that the *V-I* CMDs extend a little more than one magnitude fainter than the $B-V$ photometry.

3.1 NGC 2204

The cluster NGC 2204 [C0613-186; $6^h 13.5^m - 18^\circ 38'$ (1950)] was determined by Janes & Phelps (1994) to be 2.2 Gyr old based on estimates of the relationship between the age of the cluster and the magnitude and color differences between the turnoff and positions along the giant branch

²IRAF is distributed by the National Optical Astronomy Observatories, which is operated by the Association of Universities for Research in Astronomy, Inc., under contract to the National Science Foundation

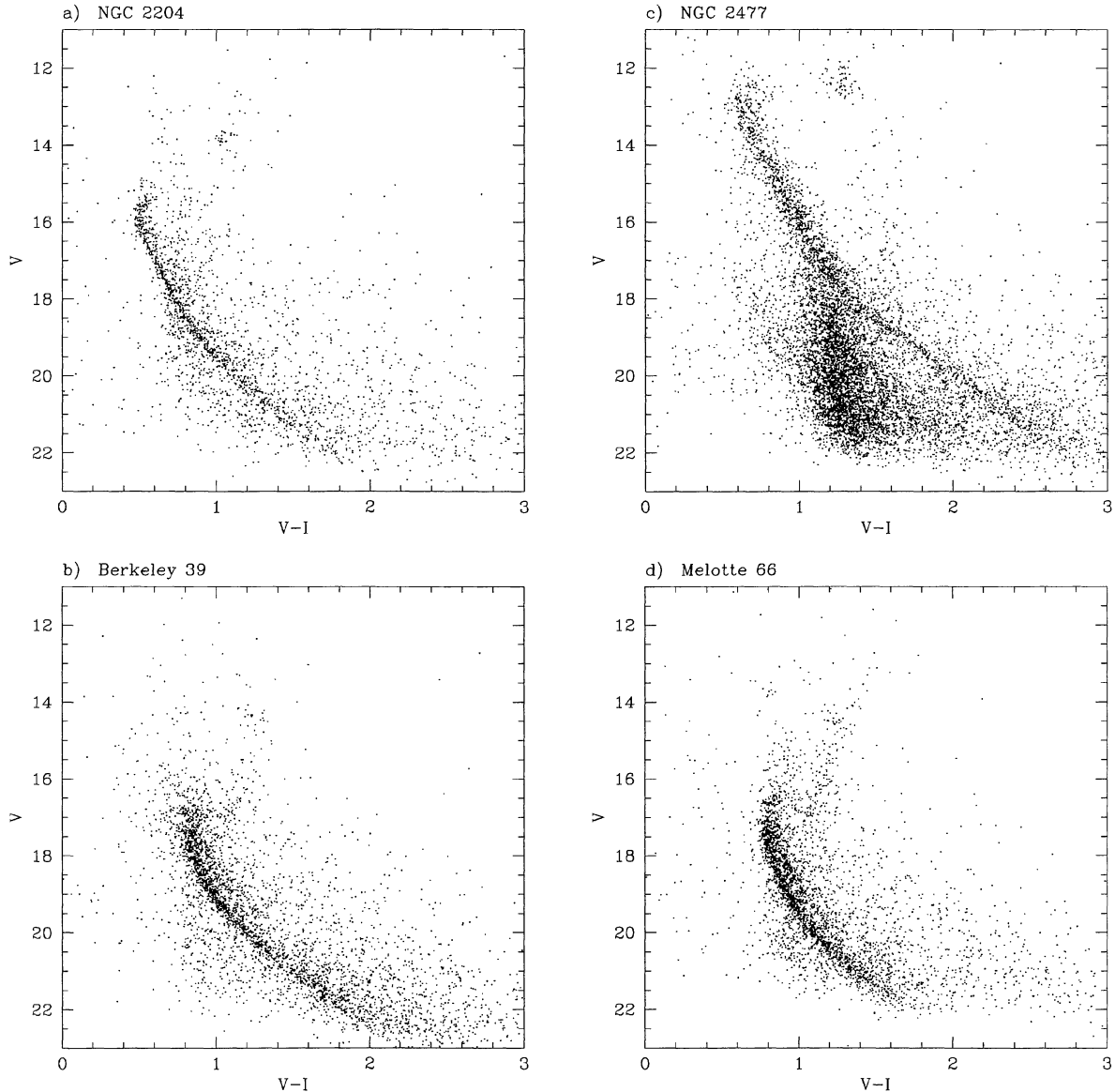


FIG. 1. CMDs of the clusters in the sample. The diagrams contain stars identified in the image and matched under the transformations for VI.

(Phelps *et al.* 1994). Hawarden (1976a) derived an age of 2.8 Gyr from isochrone comparisons to a $B-V$ CMD that went as faint as 17.5 V mag. Through isochrone comparisons, Hawarden obtained $(m-M)_o = 13.25$ mag, and from photoelectric UBV photometry and color-color diagrams, he determined $E(B-V) = 0.08$. More recently Friel *et al.* (1996) have determined reddening to the cluster based on $H\beta$ line strengths in early type stars in the field, to find $E(B-V) = 0.13 \pm 0.05$ mag.

There are a number of estimates of the metallicity of NGC 2204. Dawson (1981) determined an overall abundance of $[Fe/H] = -0.41 \pm 0.19$ from observations of the DDO CN index for 15 giants. Janes (1979) found a metallicity of -0.38 ± 0.09 from DDO photometry, and following the adjustment to a common abundance scale adopted in Janes *et al.* (1988), we increased this value by 0.08 dex to find

-0.30 ± 0.09 . Preliminary estimates of overall abundance based on moderate resolution spectroscopy of 12 giants whose radial velocities are consistent with membership, indicate an $[Fe/H] = -0.35 \pm 0.08$ (Friel & Tavaréz 1996). This new estimate agrees nicely with the earlier photometric techniques and leads us to adopt $[Fe/H] = -0.35$ as the metallicity of the cluster for the purposes of comparison to theoretical evolutionary tracks.

The NGC 2204 clump lies at $V \sim 14$ mag with the turnoff at $V \sim 15.5-16$ mag [Figs. 1(a) and 2(a)]. The deep photometry extends to $V \sim 22$ mag under the VI transformation [Figure 1(a)], nearly 4.5 magnitudes fainter than Hawarden's (1976a) photometry. This provides us with over 5 magnitudes of main sequence with which to test the models. No attempt is made to clean the CMDs in Figs. 1 or 2 of stars with large errors either in magnitude or in color that could

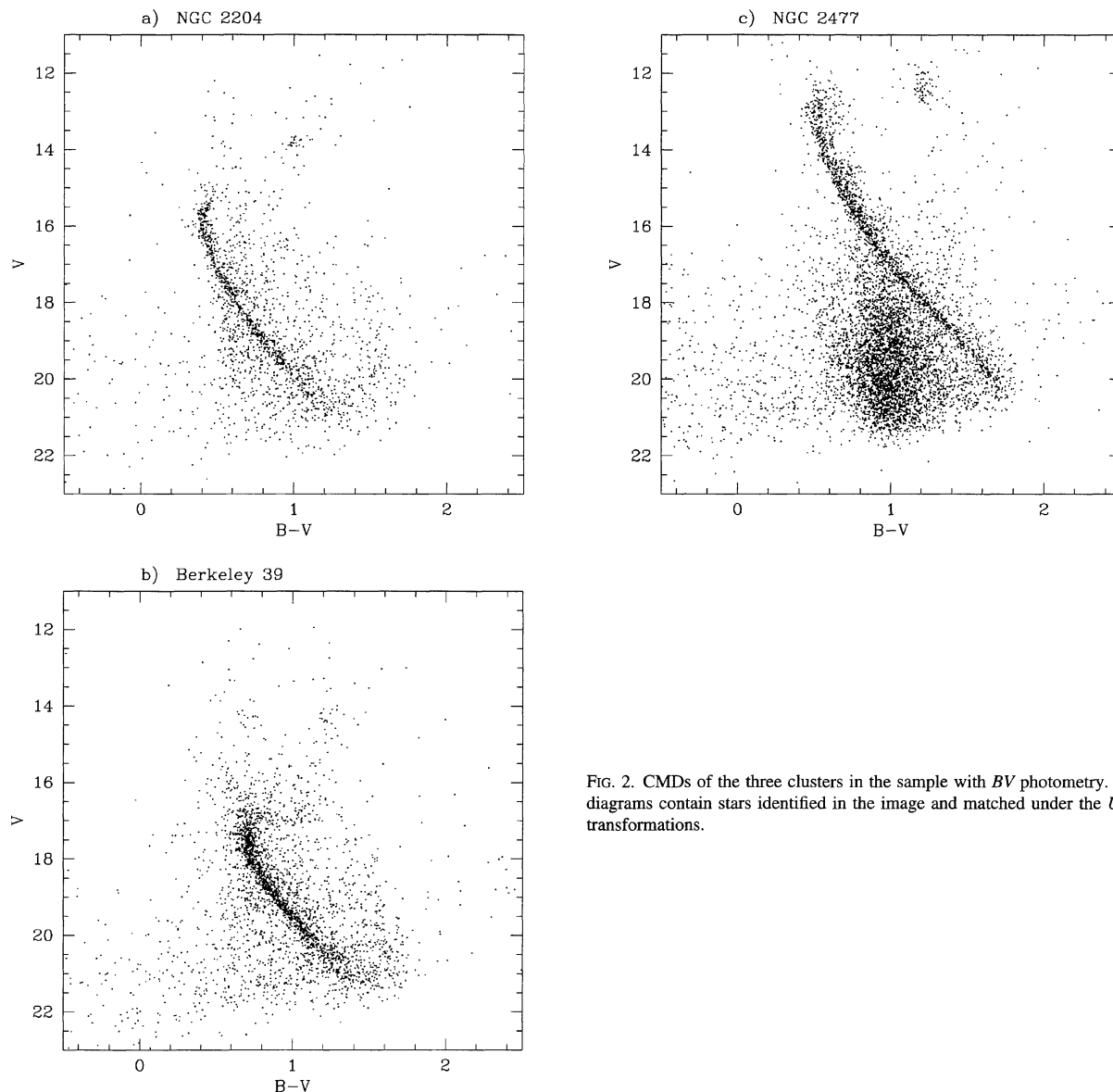


FIG. 2. CMDs of the three clusters in the sample with BV photometry. The diagrams contain stars identified in the image and matched under the UBV transformations.

result from poor matches between B , V , and I observations or from a poor psf subtraction. Because of its high galactic latitude, the field star contamination is not prominent, so CMDs of NGC 2204 appear fairly clean compared with other cluster CMDs in Figs. 1 and 2.

3.2 Berkeley 39

In their photometric study of Berkeley 39 [C0744-044; $7^h 44.2^m -4^\circ 29'$ (1950)], Kaluzny & Richtler (1989) dated the cluster at 8 Gyr with $E(B-V)=0.12$ and $(m-M)_o=13.0$ by comparing Vandenberg (1985) isochrones to a $B-V$ CMD. More recently, Carraro *et al.* (1994) determined the age, distance, and reddening from Kaluzny & Richtler's published photometry by comparing synthetic CMDs with the observed CMD of Berkeley 39. Carraro *et al.* (1994) focused on implementing synthetic CMDs in order to assess how well overshooting and standard models compare

to observed CMDs while providing homogeneous determinations of parameters of several clusters for future reference. Their preference towards models with overshooting suggest an age of 6.5 Gyr, $E(B-V)=0.10$ and $(m-M)_o=13.3$ for Berkeley 39.

The adopted metallicity of the cluster is -0.31 ± 0.08 as determined by Friel & Janes (1993) from moderate resolution spectroscopy of 7 giant stars in the cluster. An additional estimate of the reddening, $E(B-V)=0.11 \pm 0.09$, was obtained by Friel *et al.* (1996), which agrees with the two photometric analyses mentioned above.

The current study presents a $V-I$ and a $B-V$ CMD of Berkeley 39 in Figs. 1(b) and 2(b), respectively. Note that a main sequence is visible down to $V \sim 22$ in $V-I$, two magnitudes fainter than Kaluzny and Richtler (1989). Despite having more field contamination than is seen in NGC 2204 [Figs. 1(a) and 2(a)], Berkeley 39's main sequence is well

defined. At $V \sim 18$ to 20 mag, the cluster's binary sequence is visible in Fig. 1(b); however, the binary sequence is not as clearly defined in Figure 2(b). The Berkeley 39 clump is not as well defined as that of NGC 2204.

3.3 NGC 2477

The clump and turnoff for NGC 2477 [C0750-384; $7^h 50.5^m - 38^\circ 25'$ (1950)] are between 12–13 V mag in the CMDs of Figs. 1(c) and 2(c). The deep photometry extends nearly 5 magnitudes fainter than Hartwick *et al.* (1972), providing a beautiful main-sequence spanning 8 magnitudes. There is substantial field star contamination, and the field is blended with the cluster sequence near $V \sim 17.5$ mag, although the cluster sequence is well defined for fainter and brighter magnitudes.

NGC 2477 suffers from differential reddening (Hartwick *et al.* 1972), a result which probably explains the width of the upper main sequence in Figs. 1(c) and 2(c). Note that in contrast, the lower main sequence, whose slope nearly parallels the reddening line, is sharper and better defined. In their study, Hartwick *et al.* (1972) matched isochrones to a V , $B-V$ CMD corrected for the differential reddening and estimate an age of 1.5 ± 0.2 Gyr and $(m-M)_o = 10.61 \pm 0.2$. Hartwick *et al.* (1972) determined that the cluster was reddened by $E(B-V) = 0.2$ to 0.4, based on UBV photometric, photographic and intermediate-band DDO photometry, and we adopt this range for reddening values. For this study, we adopt an abundance of $[\text{Fe}/\text{H}] = -0.05 \pm 0.11$ dex determined from moderate resolution spectroscopy of seven cluster giants (Friel & Janes 1993).

3.4 Melotte 66

Figure 1(d) presents the CMD of Melotte 66 [C0724-476; $7^h 24.9^m - 47^\circ 38'$ (1950)]. The clump magnitude is near $V \sim 14.5$ with a turnoff around $V \sim 17-17.5$ mag. The main sequence is visible to magnitudes as faint as $V \sim 21-21.5$ mag. There is more field star contamination in the CMD than is observed in the CMD of NGC 2204 [Fig. 1(a)], but the main-sequence is well defined. Like Berkeley 39 [Fig. 1(b)], Melotte 66 appears to have a well populated binary sequence.

Metallicity determinations are abundant for Melotte 66. In his photometric analysis of the cluster, Hawarden (1976b) estimated $[\text{Fe}/\text{H}] = -0.39 \pm 0.18$. More recently Twarog *et al.* (1995) quoted an abundance of -0.53 ± 0.08 dex determined from UBV photometry of turnoff stars assuming $E(B-V) = 0.14 \pm 0.02$ (Dawson 1978). Friel & Janes (1993) have obtained $[\text{Fe}/\text{H}] = -0.51 \pm 0.11$ dex from 4 giants in the cluster and Olszewski *et al.* (1991) used a metallicity of -0.42 ± 0.06 dex for the cluster when they compared abundances of giants in the LMC to the metallicity of Melotte 66. Their abundance was based on the infrared calcium triplet. For this study, we adopt abundance published by Friel & Janes (1993) because their metallicities are used for the other clusters in our sample and because their results agree with the published abundances of Melotte 66.

The earliest age determinations for the cluster were made by Anthony-Twarog *et al.* (1979) and Hawarden (1976) who both dated the cluster at 6–7 Gyr. More recent photometric studies of Melotte 66 (Kaluzny & Shara 1988; Anthony-Twarog *et al.* 1994; Twarog *et al.* 1995) suggest that the main sequence of Melotte 66 has a significant width. This cannot be attributed to the field population (Kaluzny & Shara, 1988), and a number of other hypotheses have been suggested to explain the scatter in the main sequence (Anthony-Twarog *et al.* 1994). After transforming deep $b-y$ photometry from Anthony-Twarog *et al.* (1994) to a $B-V$ system, Twarog *et al.* (1995) compared a $B-V$ CMD to isochrones with convective overshooting developed by Schaerer *et al.* (1993) and estimated Melotte 66's age = 4.5 Gyr with $(m-M)_v = 13.75$, which gives $(m-M)_o = 13.3$ using the adopted reddening of 0.14 from Dawson (1978).

Two independent determinations of the cluster's reddening are available. Dawson (1978) determined a reddening of 0.14 ± 0.02 from DDO photometry of eight stars. Based on the cluster's position in the galaxy, it is possible to obtain a reddening estimate of $E(B-V) = 0.21$ from Burstein & Heiles (1982) H I maps and galaxy counts. For Melotte 66, we adopt a conservative range of reddening to the cluster based on these two determinations: 0.14 to 0.21.

In summary, we adopt the following values of abundance and reddening for clusters: For NGC 2204, $[\text{Fe}/\text{H}] = -0.35 \pm 0.08$ and $E(B-V) = 0.13 \pm 0.04$ is assumed. Berkeley 39 has a metallicity = -0.31 ± 0.08 dex and $E(B-V) = 0.11 \pm 0.09$, while NGC 2477 has a metallicity of -0.05 ± 0.11 dex and $E(B-V) = 0.2$ to 0.4. Finally, for Melotte 66 we adopt $[\text{Fe}/\text{H}] = -0.51 \pm 0.11$ and $E(B-V) = 0.14$ to 0.21. These values will be used to constrain our estimates of the ages and distance moduli when comparing isochrones to cluster CMDs.

4. ISOCHRONE COMPARISONS

For each cluster, a subset of the Bertelli *et al.* (1994) isochrones were selected based on cluster metallicity. The Bertelli *et al.* (1994) models are compared to observed CMDs because several studies give preference towards models with convective overshooting (Carraro *et al.* 1993, 1994; Twarog *et al.* 1995 to reference a few). The subset contained isochrones at three abundances chosen such that they encompassed the adopted $[\text{Fe}/\text{H}]$ value. Next we compared the subset of isochrones against a CMD of the cluster to establish the possible age range of the cluster. The ages tested ranged from 800 Myr to 12 Gyr, but most isochrones were eliminated as possible candidates because they poorly matched the turnoff region and the slope of the main sequence. Isochrones were shifted in color and magnitude in an attempt to match the turnoff and the upper main sequences in the cluster CMDs.

After the majority of the isochrones were eliminated as possible candidates, the remaining isochrones for each of the clusters were arranged in a grid of metallicity and age. Figure 3 is an example of a grid of isochrones at $[\text{Fe}/\text{H}] = 0.0, -0.4, \text{ and } -0.7$ dex for ages 2.5, 2, 1.6, and

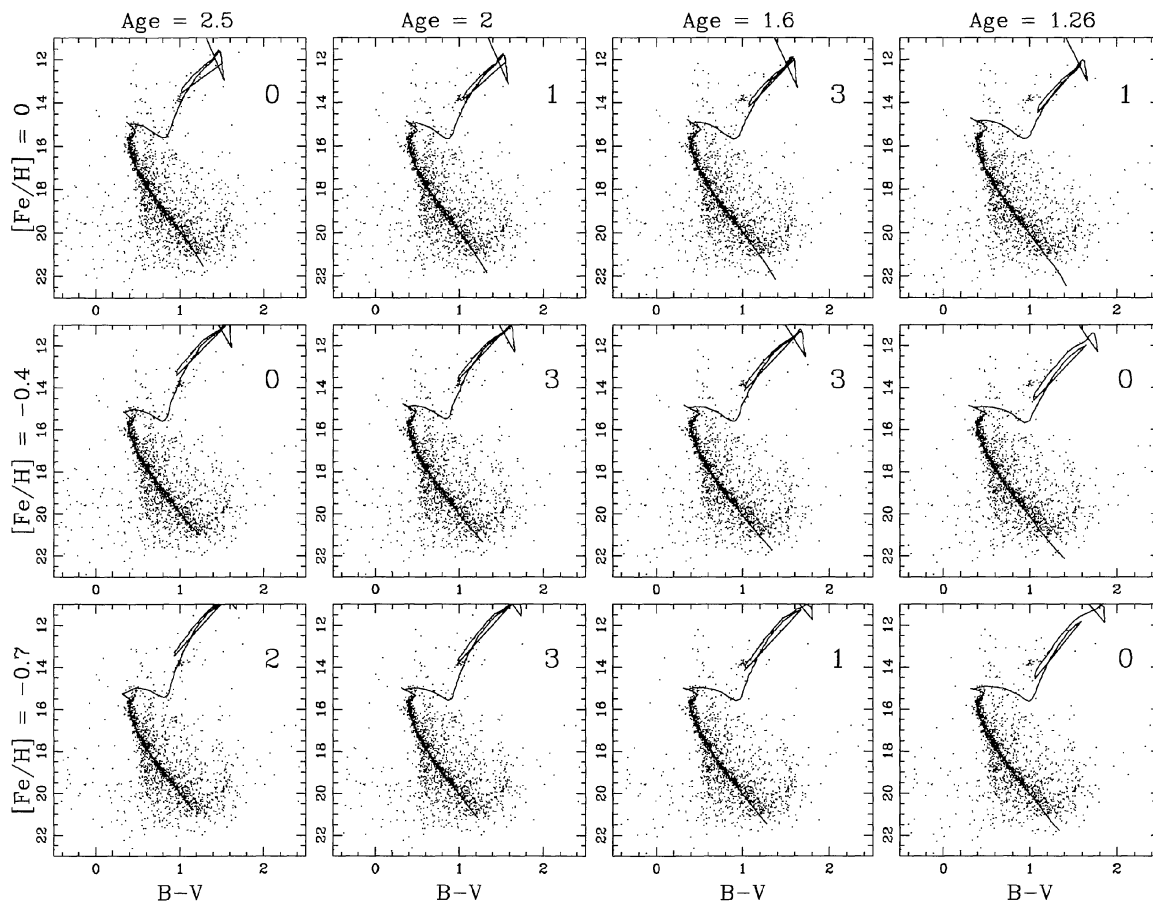


FIG. 3. A grid of isochrones is compared to NGC 2204 in a $B-V$ CMD. The grid decreases in metallicity from top to bottom and decreases in age from left to right. A number 0–3 appears in the upper right of the individual comparisons to indicate how many times the isochrone was selected as an acceptable comparison.

1.26 Gyr which was used to date NGC 2204 with the $B-V$ CMD seen in Fig. 2(a). Friel, Janes, and Kassis examined the grids independently to judge which models were acceptable matches to the data. Acceptability was based on how well the isochrones described the turnoff, lower main sequence, length and shape of the subgiant branch, and location of the red giant clump. Less emphasis was placed on the model’s ability to predict the location of the giant branch and clump.

In Fig. 3, the CMDs have been marked with a 0, 1, 2, or 3 to indicate the number of times the individual isochrones were selected as an acceptable comparison by the “judges.” Our selected models for NGC 2204 in $B-V$ begin in the lower left hand corner of the grid at $[\text{Fe}/\text{H}] = -0.7$ dex at an age of 2.5 Gyr and end with $[\text{Fe}/\text{H}] = 0.0$ dex and 1.26 Gyr. The result is a diagonal across the grid. The grid in Fig. 3 is a miniature version of the grid used to make the comparisons, and hence, subtleties used to discriminate between a good and poor match are lost. The figure demonstrates that there are several isochrones which closely follow the observed CMD and that a best fitting model should not be selected based on visual CMD comparisons alone.

The results of the fitting procedure for all clusters are summarized in Fig. 4. The metallicities of the compared iso-

chrones are plotted vertically against $E(B-V)$. In the case of V , $V-I$ CMDs, the deduced $E(V-I)$ was translated to an equivalent $E(B-V)$ by the relationship of $E(B-V) = E(V-I)/1.25$ (Dean *et al.* 1978). The individual graphs are labeled according to the cluster and either $B-V$ or $V-I$ to indicate what type of CMD was used to determine $E(B-V)$. Solid circles in Fig. 4 refer to isochrone matches which were selected by more than one judge, and hence represent comparisons that are considered to be acceptable fitting models to the CMDs (see Fig. 3 in reference to NGC 2204). The open circles represent isochrones which were selected once or not at all. Lines representing a given age were drawn and labeled in the diagrams, and the positions of these lines are determined from the metallicity and derived reddening of the matched isochrones.

Independent determinations of the metallicity and reddening exist for all clusters (see previous section). The ranges of metallicity and reddening adopted for each cluster are indicated by the hatched region in the individual graphs. Note that there is some overlap between the adopted and the derived reddening values for several isochrones for a given age and metallicity, providing constraints on these parameters. For Berkeley 39 and Melotte 66, one might imagine that the range of ages extends beyond 8 Gyr and 5 Gyr, respectively,

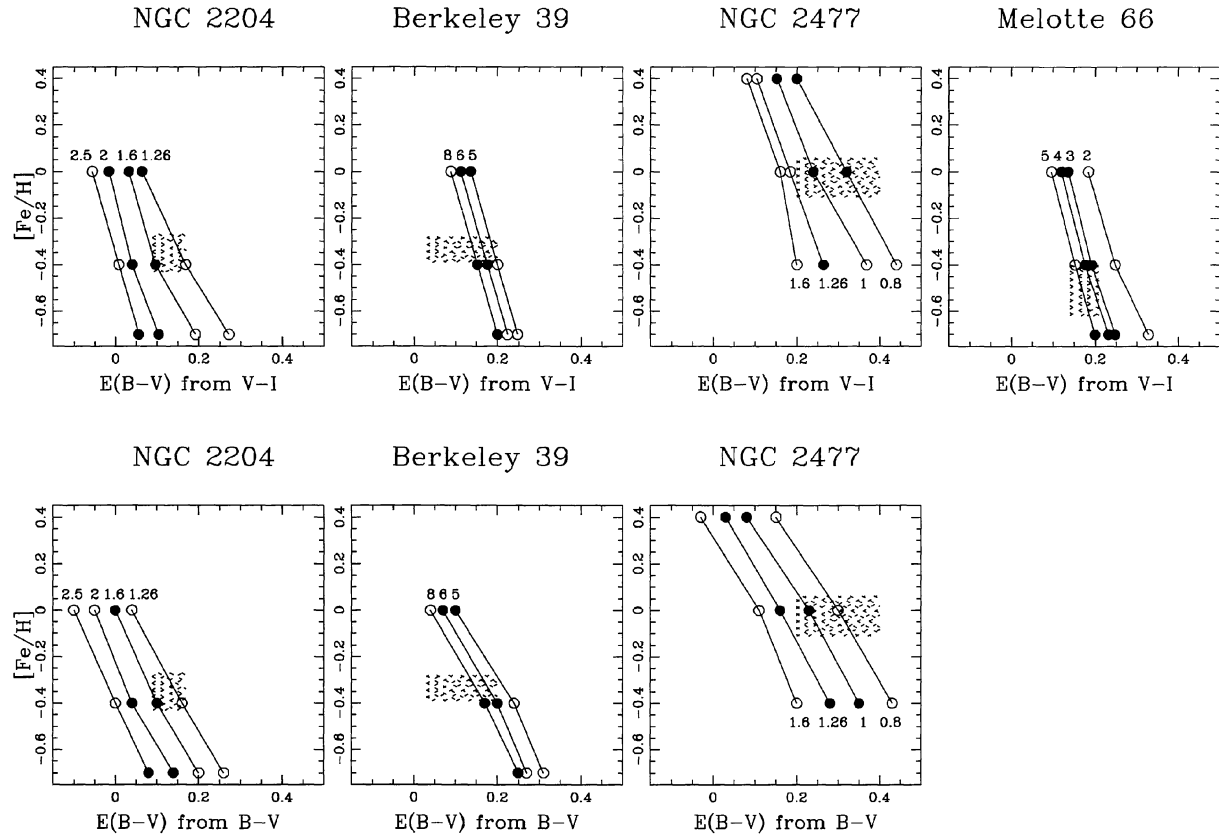


FIG. 4. For all the clusters in the sample, metallicities are plotted against reddenings determined from comparing isochrones at various ages. For three clusters, $E(B-V)$ is determined from fits to both $V-I$ and to $B-V$ CMDs. Solid lines join the results from comparisons to isochrones of a given age, as labeled. Adopted metallicities and reddenings are represented as the hatched region in the grids, which show how well the models agree with these parameters.

since the adopted values suggest that acceptable fitting models may be found at less-reddened, older ages. These isochrones, however, were obvious poor comparisons to the observed CMD, and therefore, parameter constraints provided by matching older isochrones are not presented.

Returning to NGC 2204 in $B-V$ [Fig. 2(a)] as our example for comparing isochrones, the $[Fe/H] = -0.40$ at 1.6 Gyr was selected as the best model that describes the CMD overall not only because it was selected three times as an acceptable fitting model, but because it also lay in the adopted range for the reddening and metallicity, as indicated by the hatched region in Fig. 4. The best overall isochrone match for each cluster was then used to derive the distance

modulus (see Table 2). Table 2 presents the derived ages and distance moduli for the clusters with their adopted abundances and reddenings. Acceptable models not selected as the best fitting isochrone, were used to quantify the range of age and distance modulus for each cluster. The youngest and oldest models that were selected more than once provide a lower and upper bound on the age of the cluster. The upper and lower bounds on the distance moduli (see Table 2) were calculated using the shifts in $(m-M)_v$ and $E(B-V)$ applied to match the isochrone to the CMD of the cluster. For each cluster, Table 2 also presents the distance to the Sun (D), the galactic radius (R_{gc}), and the distance from the plane of the galaxy (z).

TABLE 2. Cluster parameters.

Cluster	Metallicity [Fe/H]	$E(B-V)$	Age (Gyr)	$(m-M)_o$	D (kpc)	R_{gc} (kpc)	z dist. (pc)
NGC 2204	-0.35 ± 0.08^1	0.13 ± 0.04^2	$1.6^{+0.9}_{-0.3}$	$13.0^{+0.5}_{-0.4}$	4.0	11.1	-1100
Berkeley 39	-0.31 ± 0.08^3	0.11 ± 0.09^2	6^{+2}_{-1}	12.9 ± 0.2	3.8	11.0	700
NGC 2477	-0.05 ± 0.11^3	$0.2-0.4^2$	$1^{+0.3}_{-0.2}$	$10.5^{+0.4}_{-0.3}$	1.3	8.5	120
Melotte 66	-0.51 ± 0.11^3	$0.14-0.21^5$	4 ± 1	$13.2^{+0.3}_{-0.1}$	4.4	9.7	-1100

¹(1) Friel & Tavaréz 1996; (2) Friel *et al.* 1996; (3) Friel & Janes 1993; (4) Hartwick *et al.* 1972; (5) Dawson 1981 and Burstein & Heiles 1982.

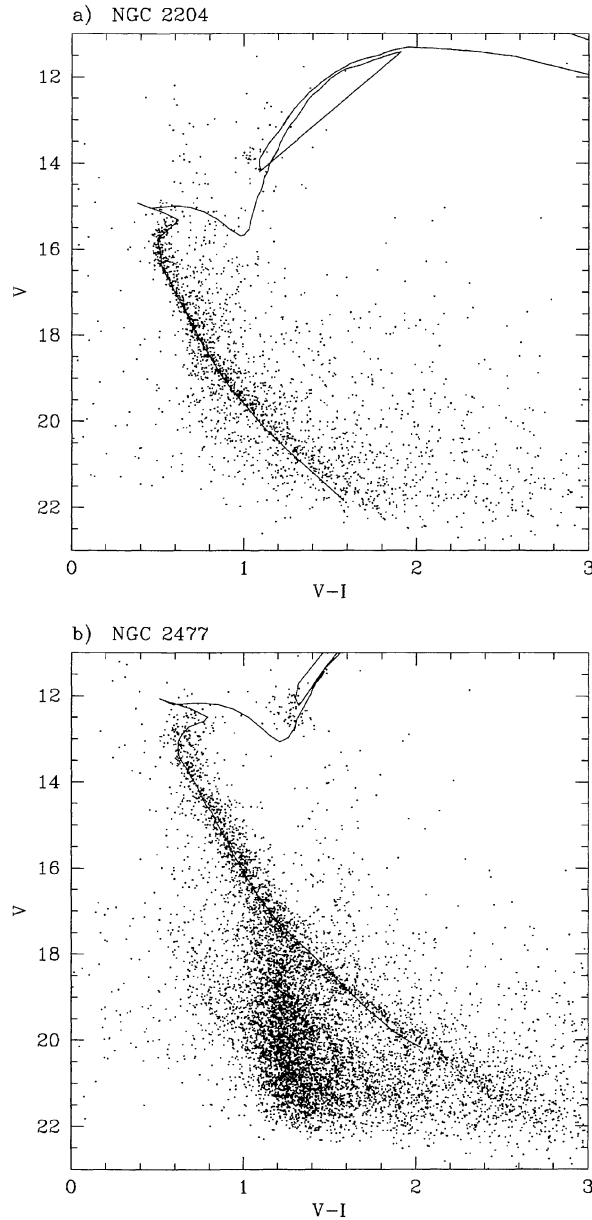


FIG. 5. The best fitting isochrones are plotted against the observed CMDs of NGC 2204 and NGC 2477. The model fit comparison to NGC 2204 has $[\text{Fe}/\text{H}] = -0.4$, $E(B-V) = 0.12$, Age = 1.6 Gyr, and $(m-M)_o = 13.0$. The best fitting model to NGC 2477 has $[\text{Fe}/\text{H}] = 0.0$, $E(B-V) = 0.24$, Age = 1 Gyr, and $(m-M)_o = 10.5$.

For NGC 2204 and NGC 2477, the isochrone matching described above was based on the CMDs presented in Figs. 1 and 2. Figures 5(a) and 5(b) present the best models compared to the $V-I$ CMDs of NGC 2204 and NGC 2477, respectively. Because of the substantial field contamination of the diagrams of Berkeley 39 and Melotte 66 in Figs. 1(b) and 1(d), the isochrone matching for these clusters was referred to CMDs computed for stars within 3.5 arcmin of the cluster centers. The cluster centers were determined by fitting Gaussian functions to the marginal distributions of the image coordinates of all stars measured. These CMDs and

the corresponding best fitting models are shown in Figs. 6(a) to 6(d).

In Fig. 6(c), there is a prominent binary sequence, which was matched with the dashed line in Fig. 6(d). The dashed line is our best fitting model shifted in magnitude by 0.7 and plotted from the turnoff through the main sequence. This shift is consistent with CMD positions assuming equal mass binaries. The binary comparison appears to describe the sequence well and crosses the best fitting model for single stars in the single star turnoff region. The main sequence of Melotte 66 appears thick at the turnoff where the best match to the binaries crosses the single-star sequence [Fig. 6(c)].

Rough estimates of the contribution due to cluster binaries by Janes & Kassis (1996) predict a 2 to 5 ratio of binaries to main-sequence stars. With this type of contribution to the color-magnitude diagram in the turnoff region, one might expect the turnoff region to be slightly scattered. It is possible that the width of the main-sequence that Kaluzny & Shara (1988) and Anthony-Twarog *et al.* (1994) address could be attributed to the binary sequence of the cluster. Certainly, more study is necessary to understand the binary population.

5. DISCUSSION AND CONCLUSION

We have compared isochrones developed by Bertelli *et al.* (1994) to the CMDs of four old open clusters: NGC 2204, Berkeley 39, NGC 2477, and Melotte 66. Ages and distance moduli were constrained using a grid of comparison isochrones. The isochrones were evaluated by Friel, Janes, and Kassis as either acceptable or unacceptable comparisons, and the ages and distance moduli were further constrained by the adopted, independently determined abundances and reddenings. Given below are cluster parameters constrained through comparing theoretical models and a brief discussion of the individual cluster CMD characteristics.

NGC 2204: Age = $1.6_{-0.3}^{+0.9}$ Gyr and $(m-M)_o = 13.0_{-0.4}^{+0.5}$. The observed CMD is not heavily contaminated by field stars and the giant and main-sequences are well defined. The best fitting model yields distances of $R_{gc} = 11.1$ kpc and $z = -1100$ pc.

Berkeley 39: Age = 6_{-1}^{+2} Gyr and $(m-M)_o = 12.9 \pm 0.2$. The clump is not well defined, and field stars contaminate the CMD. The main-sequence is well defined and extends to faint magnitudes. The best comparison places the cluster at $R_{gc} = 11.0$ kpc and 700 pc above the plane.

NGC 2477: Age = $1_{-0.2}^{+0.3}$ Gyr and $(m-M)_o = 10.5_{-0.3}^{+0.4}$. The main sequence spans a little more than 8 magnitudes and extends to lower masses than do the models. Differential reddening confuses the CMD, but the best comparison follows cluster sequences well. The best model indicates that the cluster is 8.5 kpc from the Galactic center and 120 pc above the plane.

Melotte 66: Age = 4 ± 1 Gyr and $(m-M)_o = 13.2_{-0.1}^{+0.3}$. The CMD is crowded by field stars and a prominent binary sequence may confuse the turnoff region. The single star main-sequence is well defined. The best matching model places Melotte 66 9.7 kpc from the Galactic center and -1100 pc from the plane.

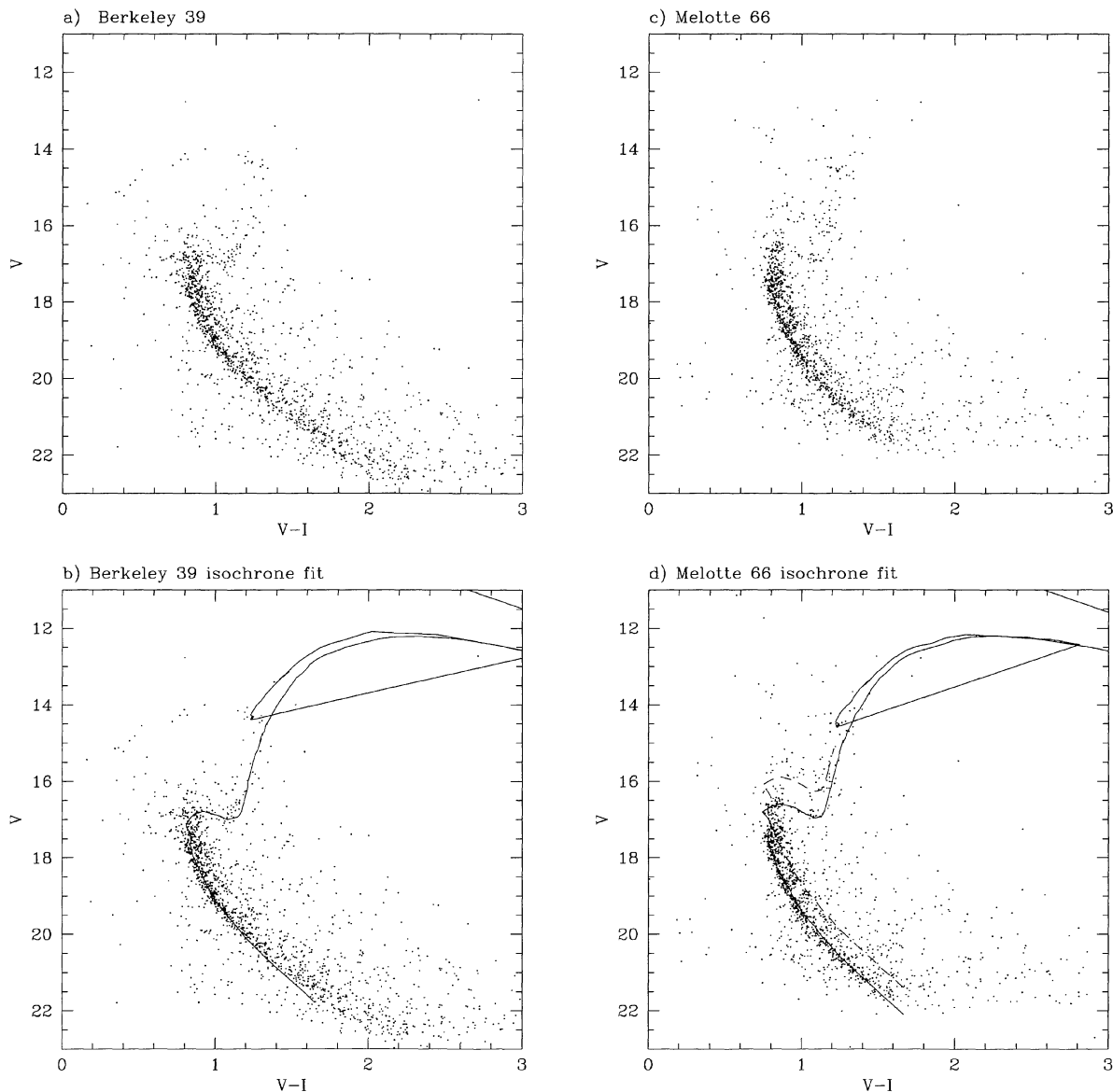


FIG. 6. CMDs “a” and “c” present the limited-area CMDs of Berkeley 39 and Melotte 66. Diagrams “b” and “d” present best fitting models (solid lines) plotted against the limited-area CMDs. Part “d” contains an additional match to the binary sequence of Mel 66 (dotted line). The best comparison to Berkeley 39 has $[\text{Fe}/\text{H}] = -0.4$, $E(B-V) = 0.18$, Age = 6 Gyr, and $(m-M)_o = 12.9$, while the best matched isochrone to Melotte 66 has a metallicity = -0.4 dex, $E(B-V) = 0.18$, Age = 4 Gyr, and $(m-M)_o = 13.2$.

In general, the models began to deviate from the observed cluster main-sequence at faint magnitudes, suggesting that for masses ~ 0.7 to $0.6M_{\odot}$, the color transformations or bolometric corrections adopted by the models may be increasingly in error relative to the observations. It is interesting that the deviations are of similar size and character in the $B-V$ and the $V-I$ colors. On the other hand, the accuracy to which the models predicted the position of the red giant clump in both color and magnitude was surprisingly good.

A comparison to the models leads to deduced reddenings and abundances that are not systematically different from those determined by independent methods. This result suggests that the zero-point of the color transformations and the inclusion of overall abundances and their resultant opacity

sources in the models are generally consistent with the observed scales. Overall, the models are quite successful at reproducing the majority of features in the observed cluster color-magnitude diagrams.

The photometry for all clusters in this study is available upon request.

This study was supported by a Willamette University 1996 Carson Undergraduate Research Grant, the National Science Foundation Grant AST-9315300 to Boston University, and NSF REU Grant AST-9300391 to the Maria Mitchell Observatory. The authors also wish to thank Andrew Layden for his help with the preliminary processing of the data. Thanks are also extended to students of Boston University.

REFERENCES

- Anthony-Twarog, B. J., & Twarog, B. A. 1985, *ApJ*, 291, 595
 Anthony-Twarog, B. J., Twarog, B. A., & McClure, R. D. 1979, *ApJ*, 233, 188
 Anthony-Twarog, B. J., Twarog, B. A., & Sheeran, M. 1994, *PASP*, 106, 486
 Bertelli, G., Bressan, A., Chiosi, C., Fagotto, F., & Nasi, E. 1994, *A&A*, 106, 275
 Burstein, D., & Heiles, C. 1982, *AJ*, 87, 1165
 Carraro, G., Bertelli, G., Bressan, A., & Chiosi, C. 1993, *A&AS*, 101, 381
 Carraro, G., Chiosi, C., Bressan, A., & Bertelli, G. 1994, *A&AS*, 103, 375
 Dawson, D. W. 1978, *AJ*, 83, 1424
 Dawson, D. W. 1981, *AJ*, 86, 237
 Dean, J. F., Warren, P. R., & Cousins, A. W. J. 1978, *MNRAS*, 183, 569
 Friel, E. D. 1995, *ARA&A*, 33, 381
 Friel, E. D., & Janes, K. A. 1993, *A&AS*, 267, 75
 Friel, E. D., Miller, N., Hong, L. N., & Janes, K. A. 1996, *PASP* (submitted)
 Friel, E. D., & Tavaréz, M. 1996, in preparation
 Gozzoli, E., Tosi, M., Marconi, G., & Bragaglia, A. 1996, *MNRAS* (in press)
 Hartwick, F. D. A., Hesser, J. E., & McClure, R. D. 1972, *ApJ*, 174, 557
 Hawarden, T. G. 1976a, *MNRAS* 174, 225
 Hawarden, T. G. 1976b, *MNRAS*, 174, 471
 Janes, K. A. 1979, *ApJS*, 39, 139
 Janes, K. A., & Kassis, M. 1996, in Third Pacific Rim Conference on Recent Developments on Binary Star Research, edited by K.-C. Leung (*PASP Conf. Series*) (in press)
 Janes, K. A., & Phelps, R. L. 1994, *AJ*, 108, 1773
 Janes, K. A., Tilley, C., & Lynga, G. 1988, *AJ*, 95, 771
 Kaluzny, J. 1994, *AcA*, 44, 247
 Kaluzny, J., & Richtler, J. 1989, *AcA*, 39, 139
 Kaluzny, J., & Shara, M. M. 1988, *AJ*, 95, 785
 Kassis, M., Friel, E. D., & Phelps, R. L. 1996, *AJ*, 111, 820
 Landolt, A. 1992, *AJ*, 104, 340
 MacMinn, D., Phelps, R. L., Janes, K. A., & Friel, E. D. 1994, *AJ*, 107, 1806
 Montgomery, K. A., Marschall, L. A., & Janes, K. A. 1993, *AJ*, 106, 1079
 Montgomery, K. A., Janes, K. A., & Phelps, R. L. 1994, *AJ*, 108, 585
 Olszewski, E. W., Schommer, R. A., Suntzeff, N. B., & Harris, H. C. 1991, *AJ*, 101, 515
 Phelps, R. L., Janes, K. A., & Montgomery, K. A. 1994, *AJ*, 107, 1079
 Phelps, R. L., Janes, K. A., Friel, E. D., & Montgomery, K. A. 1995, in the *Formation of the Milky Way*, edited by E. A. Alfaro (Cambridge University Press, Cambridge), p. 187
 Phelps, R. L., & Janes, K. A. 1996, *AJ*, 111, 1604
 Schaefer, D., Meynet, G., Maeder, G., & Schaller, G. 1993, *A&AS*, 98, 523
 Twarog, B. A., Anthony-Twarog, B. J., & Hawarden, T. G. 1995, *PASP*, 107, 1215
 VandenBerg, D. A. 1985, *ApJS*, 58, 711